# Low-temperature fluid-phase behavior of ST2 water

Yang Liu, Athanassios Z. Panagiotopoulos, and Pablo G. Debenedetti[a)]
*Department of Chemical Engineering, Princeton University, Princeton, New Jersey 08544, USA*

(Received 30 July 2009; accepted 25 August 2009; published online 11 September 2009)

We perform histogram-reweighting Monte Carlo simulations of the ST2 model of water in the grand-canonical ensemble in order to investigate its low-temperature fluid-phase behavior. Using Ewald summation treatment of long-range electrostatic interactions, we locate the critical point of the liquid-liquid transition at $T=237\pm4$ K, $\rho=0.99\pm0.02$ g/cc, $P=167\pm24$ MPa. Contrary to previous reports in the literature [Brovchenko *et al.*, J. Chem. Phys. **118**, 9473 (2003); Brovchenko *et al.*, J. Chem. Phys. **123**, 044515 (2005)], according to which there are three liquid-liquid transitions in ST2 with simple truncation of electrostatic interactions, and two in ST2 with reaction field treatment of long-range Coulombic forces, we find only one liquid-liquid transition. Our work points to the sensitivity of results to the proper treatment of electrostatic interactions, and to the introduction of artificial constraints that limit the magnitude of density fluctuations. © *2009 American Institute of Physics*. [doi:10.1063/1.3229892]

## I. INTRODUCTION

Water is the most abundant liquid on earth, and the only substance that occurs naturally in the solid, liquid, and vapor phases.[1] Its properties affect virtually every aspect of our lives, including climate, agriculture and public health, and have a profound influence on the chemical processes that are essential for life.[1] It is difficult to think of an industrial process that does not involve water as a solvent, reactant, product, or impurity.[2]

Water's well-known oddities include its uncommonly high (for a nonmetallic hydride) melting and boiling temperatures; the fact that, if sufficiently cold, the liquid expands and becomes more compressible when cooled, and less viscous when compressed; and its large number of crystal polymorphs (at least 13, of which four are metastable and nine are stable over a range of temperatures and pressures).[3,4] Liquid water's anomalies become more pronounced when it is cooled below the freezing point without crystallizing (supercooled).[2] In an important paper, Poole *et al.*[5] proposed that supercooled water has a liquid-liquid critical point in addition to the ordinary vapor-liquid critical point. This suggestion has proved to be particularly fruitful because it provided a thermodynamically consistent framework for interpreting a large number of experimental observations, including the possibility that water possesses two distinct glassy phases, separated by a first-order phase transition.[6] According to the two-critical-point scenario of Poole *et al.*,[5] water's second critical point is the end-point of the first-order transition between two liquids (low-density and high-density liquid, respectively), of which the corresponding transition between distinct glasses[6,7] [low-density amorphous (LDA) ice and high-density amorphous (HDA) ice] is the structurally arrested manifestation. Alternative thermodynamic interpretations of water's metastable, low-temperature behavior have been proposed.[8,9] The suggestion that a pure substance can have additional, distinct disordered phases, separated by a first-order transition, in addition to the ordinary vapor-liquid transition, is commonly referred to as liquid (or vitreous) polyamorphism.[10–13] In addition to water, substances for which evidence of polyamorphism has been reported include silicon,[14,15] germanium,[16] phosphorus,[17] sulfur,[18] and triphenyl phosphite.[19–22]

Evidence consistent with the existence of a liquid-liquid critical point in water suggests that it is located deep inside the metastable region, where the stable state of water is crystalline[23] (e.g., ~1 kbar and 220 K). The experimental challenges associated with performing careful physical property measurements on highly metastable samples (which would be needed to unambiguously prove the existence of a critical point) are considerable. This has led to two strategies: one experimental and one computational. Experimental studies have exploited the suppression of ice nucleation when water is confined in ~20 Å hydrophilic pores.[24–32] Much has thereby been learned about the properties of cold liquid water in nanoscale confinement. Relating this knowledge to bulk water behavior, however, remains an important challenge.[33] Computational studies, on the other hand, have sought to investigate water's metastable phase behavior by exploiting the highly improbable occurrence of a crystal nucleation event in the course of a regular molecular dynamics or Monte Carlo simulation of any of the existing models of water in the bulk. This easy computational access to deeply supercooled states has enabled a number of studies of the metastable phase behavior of various molecular water models, aimed at gaining fundamental understanding of the relationship between the calculated physical properties, including the presence of polyamorphic transitions,[34–39] and the models' underlying characteristics (e.g., geometry; magnitude and location of electrostatic charges; internal degrees of freedom, etc.).

More than thirty years after its introduction, the ST2

[a)]Author to whom correspondence should be addressed. Electronic mail: pdebene@princeton.edu.

 

model[40] continues to play an important role in computational studies of water. This potential tends to enhance tetrahedral order, and hence exhibits waterlike anomalies up to higher temperatures than real water. For example, ST2 water's density maximum at atmospheric pressure occurs at ~330 K (Ref. 41) (versus 277 K in actual water). This enables the study of waterlike anomalies at comparatively high temperatures, when relaxation rates are not prohibitively slow. In contrast, the SPC/E model[42] of water exemplifies the "understructured" case, whereby anomalies are displaced to low temperatures, making computational exploration of polyamorphism more difficult.

In 2003 Brovchenko *et al.*[43] proposed that ST2 water exhibits multiple liquid-liquid transitions. This intriguing result generated considerable interest, as did a subsequent study by these same authors,[44] suggesting the existence of multiple polyamorphic transitions in the SPC/E,[42] TIP4P,[45] and TIP5P (Ref. 46) models water. Most of the calculations of Brovchenko *et al.*[43] used a simple spherical truncation of electrostatic interactions, without long-range corrections (for the ST2 model, both simple truncation[43] and reaction field[47] long-range correction of Coulombic interactions[44] were considered). Although simple truncation was used in the original parametrization of these models, it is well-known that failure to implement long-range corrections to truncated electrostatic interactions leads to severe distortions of calculated structural properties.[48,49] Long-range correction of electrostatic interactions is routinely done, either through the reaction field or Ewald summation methods.[50] In this work, as explained in detail in Sec. II, we use the Ewald summation method. Brovchenko *et al.*[43] used constrained ensemble simulations[51] that suppress density fluctuations to detect polyamorphic phase transitions. As explained in detail in Sec. II, we use a histogram-reweighting approach,[52] which does not impose artificial constraints and allows the accurate determination of phase coexistence properties. The main conclusion from the present work is that we see no evidence of multiple liquid-liquid phase transitions, highlighting the sensitivity of polyamorphic phase transitions involving modest density changes to the treatment of electrostatic interactions, and possibly also to the artificial suppression of density fluctuations. The use of state-of-the-art techniques for the calculation of phase coexistence, furthermore, allows us to locate the critical point corresponding to the ST2 model's liquid-liquid transition with considerably greater accuracy than has hitherto been possible.

It should be emphasized that our choice of model potential is motivated not by its inherent accuracy in modeling water, but by the reports in the literature of multiple liquid-liquid transitions in ST2 water.[43,44] The fact that the hypothesis of a second, metastable critical point in supercooled water was formulated in pioneering work using ST2 water[5] was also a factor in our choice of this model for the first application of state-of-the-art computational methods to the problem of liquid-liquid equilibrium in supercooled water. That said, it is important to note that the ST2 model with either reaction field or Ewald treatment of long-range electrostatic interactions underpredicts liquid water's density at ambient conditions by a significant amount: at 300 K and 1 bar the computed values are 0.92 g/cc (Ewald; this work), 0.92 g/cc (reaction field; Ref. 44 and references cited therein), 1 g/cc (truncation; Ref. 44 and references cited therein).

This paper is structured as follows. Methodological details are provided in Sec. II. Results and discussion are presented in Sec. III. The major conclusions of this work, as well as some directions for future inquiry suggested by this study, are presented in Sec. IV.

## II. METHODS

### A. Model system

In the ST2 model,[40] each water molecule has a tetrahedral structure, with an oxygen atom at the center and four point charges (two positive charges representing partially shielded protons and two negative charges) located at the vertices. The distances to the oxygen from a positive charge and from a negative charge are 1 and 0.8 Å, respectively. Oxygen-oxygen interactions are described using the Lennard-Jones potential with a characteristic distance $\sigma = 3.10$ Å and a characteristic energy $\varepsilon = 0.316\,94$ kJ/mol. The Coulombic interactions between the charges are supplemented with a modulation function that varies smoothly between 0 at small distance and 1 at large distance. In our study, the simulations were carried out in a cubic box of length $L = 18.6$ Å $(6\sigma)$. Periodic boundary conditions were applied in the $x$, $y$, and $z$ directions. We used a cutoff at $r = 7.75$ Å $(2.5\sigma)$ for the Lennard-Jones interactions between oxygen atoms. The long-range Coulombic interactions between the charged sites of water molecules were calculated using the Ewald summation. The long-range corrections for the Lennard-Jones potential were negligible compared to the corresponding electrostatic interactions, and were therefore not included in our calculation. The parameter describing the width of the screening charge Gaussian distribution in the Ewald summation was set to be 0.269 $Å^{-1}$, and 518 wave vectors were used in the reciprocal space sum.

### B. Histogram-reweighting grand-canonical Monte Carlo

Monte Carlo simulations in the grand-canonical ensemble were used for the computation of phase coexistence. Input parameters to the simulations were the temperature $T$, volume $V$, and chemical potential $\mu$. In what follows, we use a dimensionless chemical potential $\mu^*$, defined as

$$\mu^* = \frac{1}{\varepsilon}(\mu^{\mathrm{ex}} + k_B T \ln \rho\sigma^3) = \frac{1}{\varepsilon}\left(\mu + k_B T \ln \frac{\sigma^3}{\Lambda^3}\right), \tag{1}$$

where $\varepsilon$, $\sigma$ are the characteristic parameter values of ST2 water, $\Lambda$ is the thermal de Broglie wavelength, $k_B$ is Boltzmann's constant, and $\mu^{\mathrm{ex}}$ is the difference between the chemical potential and that of an ideal gas at the same $T$ and density $\rho$.

Microstates were generated with molecule displacement, rotation, insertion or deletion moves. Metropolis criteria[53] were applied for accepting or rejecting moves. In displacement moves, a randomly selected molecule was displaced by an amount uniformly distributed between $-3\sigma/40$ and

$+3\sigma/40$ along each of the coordinate directions. In rotation moves, a randomly selected molecule was rotated by an amount uniformly distributed between $-2\pi/5$ and $+2\pi/5$ about one of the three space-fixed axes chosen at random. The acceptance ratio was roughly 25% on average for displacement moves, and about 28% for rotation moves. Molecules were inserted at random positions and with random orientation. At each step, the ratio of the probabilities of attempting displacement, rotation, insertion, or deletion moves was 1:1:10:10. After equilibrium was reached, data for the probability $f(N,U)$ of occurrence of $N$ particles with total configurational energy in the vicinity of $U$ was collected and histograms were generated. The bin width of the energy was $\Delta U=8\varepsilon$. Several sampling difficulties involved in the search for the liquid-liquid transition should be pointed out. First, the liquid-liquid transition is located in the deeply supercooled region ($\leq$237 K), where the mobility of the water molecules is low, resulting in a decreased efficiency in the sampling of phase space. Specifically, the high density and low temperature of the system cause most molecular insertion/deletion attempts to fail, since there is a high probability of overlap in insertion attempts, as well as an energy increase caused by deleting a molecule without a subsequent structural relaxation. The acceptance ratio for molecular insertions/deletions over the range of conditions examined ranged from 0.001% to 0.01%. In addition, the difference in densities between the coexisting liquid phases, which is the key parameter used to detect a phase transition, is quite small. Consequently, sufficiently long sampling must be performed in order to obtain reproducible histograms, and caution must be exerted to distinguish real phase transitions from histogram sampling noise.

We first performed 268 parallel independent runs, including 56 runs at $T=244.2$ K and chemical potential $\mu^*=-79.88$, 56 runs at $T=242.3$ K and $\mu^*=-80.5$, 100 runs at $T=240.0$ K and $\mu^*=-80.33$, and 56 runs at $T=228.6$ K and $\mu^*=-81.9$. These runs covered the density range $0.90\leq\rho\leq1.15$ g/cm$^3$, and early tests showed that the liquid-liquid phase transition was likely to occur across this temperature and density range. Several initial configurations with different densities were prepared and equilibrated at the above conditions, and the final configurations from earlier runs were selected randomly to be the initial configurations of subsequent runs. Each run consisted of $10^9$ production steps. Each single run only partially sampled the probability distribution of the system at that specific condition and produced a very noisy histogram, because of the small acceptance ratio for additions and removals. Using histogram-reweighting techniques,[54] we combined all the histograms and reweighted to the conditions of interest, as long as the ranges of density and energy were covered. Specifically, when data from multiple runs were combined, we used the technique developed by Ferrenberg and Swendsen[52] to determine the optimal amount by which to shift the raw data in order to obtain a global free energy function. Following this procedure, we obtained the histogram information covering the broad temperature and density range 228.6 K$\leq T\leq$244.2 K and 0.90 g/cm$^3\leq\rho\leq$1.15 g/cm$^3$, respectively. To make sure that the sampling was enough for the combined histograms to reflect the true probability distribution of the system, the self-consistency of the histograms was checked as follows. First, we compared the histograms generated by randomly removing thirty runs and combining the remaining runs. Second, we reweighted the histograms resulting from combining the runs at a single temperature $T=244.2$ K, $T=240.0$ K, $T=242.3$ K, and $T=228.6$ K, respectively, to selected common thermodynamic conditions, and compared the resulting histograms. Using these tests we verified that the histograms were indeed self-consistent. The consistency of the number and the location of the peaks in the histograms confirmed the existence of true phase transitions. The simulations required a total of approximately 10 CPU years on 3 GHz Xeon processors.

Motivated by the work of Brovchenko *et al.*,[43,44] reporting three liquid-liquid transitions in ST2 water with simple truncation of electrostatic interactions, and two liquid-liquid transitions in the ST2 model with reaction field treatment of long-range Coulombic interactions, we further explored the histograms with the density range expanded to 1.30 g/cm$^3$ at a single temperature $T=217.2$ K, which lies well below the critical points reported by Brovchenko *et al.*[44] Several runs starting with different densities were first equilibrated at $\mu^*=-84.5$ and $-83.5$ to detect other possible liquid-liquid transitions in the density range 0.90 g/cm$^3\leq\rho\leq$1.20 g/cm$^3$. The obtained information was checked with the histograms reweighted from higher temperatures. To obtain the histogram within the density range 1.20 g/cm$^3\leq\rho\leq$1.30 g/cm$^3$, the final configurations which satisfied $\rho>1.0$ g/cm$^3$ from previous simulations were chosen randomly as initial configurations and were equilibrated at $\mu^*=-83.5$, $-82.5$, respectively. After equilibration was achieved, we started with the new equilibrated configurations and performed 19 runs at $\mu^*=-83.5$, and 25 runs at $\mu^*=-82.5$, each consisting of 1000 million production steps. Histograms at these conditions were generated, combined and reweighted to other chemical potentials. As will be explained in Sec. III, the histograms exhibited a single sharp peak in the chemical potential range $-83.5\leq\mu^*\leq-82.5$, corresponding to the density range of interest, 1.20 g/cm$^3\leq\rho\leq$1.30 g/cm$^3$. Furthermore, an additional run in the *NVT* ensemble at $T=217.2$ K and $\mu^*=-83.5$ was performed to check the diffusivity of the system. Although the mobility was low, the system was found to be diffusive. The mean-squared displacement was found to vary linearly with the number of steps after a sufficient number of steps, at a rate of approximately $0.33\sigma^2$ per million steps.

### C. Determining the critical point

Finite-size scaling theory[55,56] has been widely used in studying the critical behavior of Lennard-Jones fluids,[57] lattice polymers,[58] binary mixtures,[59] the restricted primitive model,[60] and tetrahedrally coordinated functionalized colloids.[61] In this work, we also use this approach for the determination of critical parameters. For one-component systems, the ordering operator, $M$, is defined as a linear combination of the number of particles $N$ and total configurational energy $U$

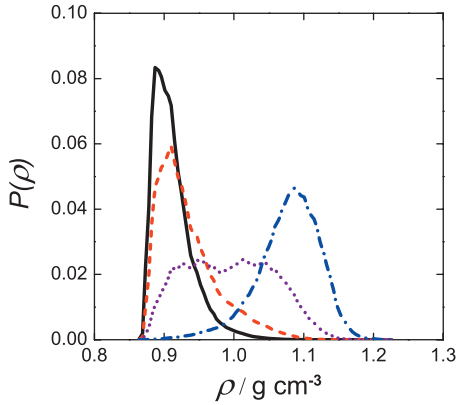


FIG. 1. Density histograms for ST2 water at 244.2 K. Black solid line: $\mu^*=-81.5$; red dashed line: $\mu^*=-81.0$; purple dotted line: $\mu^*=-80.4$; blue dash-dotted line: $\mu^*=-79.6$.

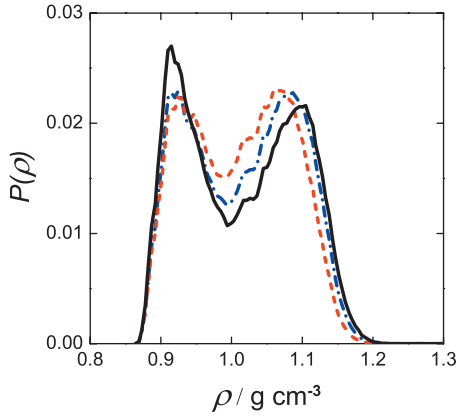


FIG. 2. Histograms indicating the liquid-liquid phase transition in ST2 water. Red dashed line: $T=241.9$ K, $\mu^*=-80.5$; blue dash-dotted line: $T=240.0$ K, $\mu^*=-80.6$; black solid line: $T=238.1$ K, $\mu^*=-80.7$.

$$M = N - sU, \tag{2}$$

where $s$ is the field mixing parameter. At criticality, the probability distribution for a given system, $P(x)$, where the scaling parameter $x$ is given by $x=A(M-M_c)$, has a universal form. The nonuniversal parameter $A$ and the critical value of the ordering operator $M_c$ are chosen so that zero mean and unit variance of the distribution are observed in the scaling parameter. A precise probability distribution of the order parameter for the three-dimensional (3D) Ising-model universality class can be found elsewhere.[62] It is believed that the liquid-liquid critical point also belongs to the Ising universality class, like the ordinary liquid-gas critical point.[61] To obtain the critical parameters for the liquid-liquid transition of ST2 water, we adjusted the chemical potential, temperature and field mixing parameter $s$ so as to achieve the best fit to the 3D universal distribution. This allowed us to determine the liquid-liquid critical point with considerably higher precision than has hitherto been possible.

The critical pressure was estimated separately using the volume fluctuation method of Harismiadis *et al.*[63] Several simulations in the $NVT$ ensemble, starting from equilibrated configurations near the critical point, were conducted and energy was calculated every 4 steps at a volume $(V')$ slightly larger than the volume of our simulation box $(\Delta V \approx 0.003$ V). The pressure is then obtained from the following expression:[63]

$$\frac{P}{k_BT} = \frac{N}{V} + \frac{1}{\Delta V}\ln\left\langle \exp\left(-\frac{\Delta U}{k_BT}\right)\right\rangle, \tag{3}$$

where $\Delta U = U_{V'} - U_V$ and $\langle\cdots\rangle$ denotes the thermal average in the $NVT$ ensemble.

## III. RESULTS AND DISCUSSION

Figures 1 and 2 show the density probability distribution at different temperatures and chemical potentials spanning conditions where the liquid-liquid transition of ST2 water is observed. Figure 1 illustrates the change in the observed histogram upon increasing the chemical potential at a single temperature, $T=244.2$ K. The histogram evolves from a single sharp peak at $\rho \approx 0.9$ g/cm$^3$ to another single peak at $\rho \approx 1.1$ g/cm$^3$, while at intermediate values of the chemical potential the system samples states on both sides of the transition, resulting in a comparatively flat histogram. This is typical of near-critical behavior. Reweighted to lower temperatures, the histograms exhibit sharper peaks that clearly show this phase transition between low-density and high-density liquid phases (Fig. 2). The histogram data were then matched to the 3D Ising universal distribution and critical parameters were determined. Eight independent matches to the 3D Ising distribution were conducted by randomly combining one, two, three, or four subsets of runs to check the consistency of our results. Each subset of runs was comprised of simulations performed at the same temperature. An example of our fitting is shown in Fig. 3. From this analysis, we conclude that the critical point of the liquid-liquid transition for ST2 water is located at $T_c=237\pm4$ K, $\mu_c^*=-80.9\pm0.4$, $\rho_c=0.99\pm0.02$ g/cm$^3$, and field mixing parameter $s=-0.006\pm0.001$. The uncertainties were calculated from the standard deviations of the eight independent data sets, multiplied by two. The critical pressure is $P_c=167\pm24$ MPa, which was calculated in $(N,V,T)$ simulations at 240 K and 0.99 g/cc using the method described in Sec. II C. The uncertainty was calculated from the standard deviations of five independent parallel runs, multiplied by two. The location of the critical point for this liquid-liquid

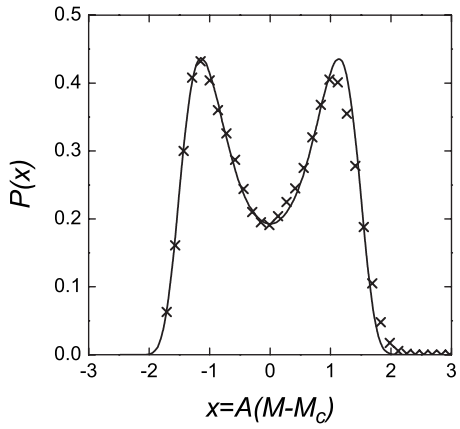


FIG. 3. Matching of the probability distribution, $P(x)$, to the 3D Ising universality class, indicated by solid line. Crosses are our results.

TABLE I. Critical parameters of the liquid-liquid transition for ST2 water [The critical parameters from Brovchenko *et al.* (Ref. 44) shown here correspond to the lowest-density liquid-liquid transition in that paper.]

| | Poole *et al.*[a] | Brovchenko *et al.*[b] | | This work |
|---|---|---|---|---|
| Treatment of long-range electrostatic interactions | Reaction field | None | Reaction field | Ewald sum |
| $T_c$/K | 245 | $\sim 290 > T_c > 275$ | $\gtrsim 260$ | $237 \pm 4$ |
| $\rho_c$/gcm$^{-3}$ | 0.94 | ~0.95 | ~0.97 | $0.99 \pm 0.02$ |
| $\mu_c^*$ | — | — | — | $-80.9 \pm 0.4$ |
| $P_c$/MPa | 180 | Negative | ~130 | $167 \pm 24$ |

[a]Reference 37.
[b]Reference 44.

transition has been estimated by previous simulation studies.[37,44] These results, as well as our calculation, are shown in Table I. Poole *et al.*[37] performed a high-resolution molecular dynamics simulation of the equation of state of ST2 water in the *NVT* ensemble and located the critical point by tracing the spinodal lines of both the low-density and the high-density liquid (see, however, Ref. 64 for a discussion of finite-size effects in the calculation of spinodals). Brovchenko *et al.*[44] provided an approximate location of the liquid-liquid transitions using Monte Carlo simulations in the restricted *NPT* ensemble as well as the Gibbs ensemble. It can be seen from Table I that our critical temperature is considerably lower than the results of Brovchenko *et al.*,[44] but is close to the estimate by Poole *et al.*[37] Our estimate of the critical pressure is also in agreement with the result of Poole *et al.*[37] The estimates of the critical density from the three studies are in reasonable agreement.

In order to estimate finite-size effects on the critical parameter values, we performed simulations employing a smaller system size, $L=5\sigma$ (versus $L=6\sigma$ throughout the rest of this work, which is to say a volume reduction by a factor of 0.58). The critical point values determined using this smaller system size after 60 runs at 240 K and $\mu^*=-80.7$, each consisting of $10^8$ equilibration and $10^9$ production steps, were $T_c=235$ K, $\mu_c^*=-81$, and $\rho_c=0.99$ g/cc. Although we did not attempt a systematic investigation spanning a broader range of system sizes because of the severe computational demands associated with such a calculation (see Sec. II B), the good agreement between the $L=5\sigma$ and $L=6\sigma$ results lends confidence to the accuracy of the critical parameters reported in Table I.

The criteria for phase coexistence are equality of temperature, chemical potential, and pressure. The first two constraints are satisfied by construction, and the integral under the density probability distribution is proportional to the pressure. By matching the areas under the low-density liquid and high-density liquid portion of the histogram, we calculated the phase coexistence curve away from the critical point. This is shown in Fig. 4. In order to obtain the phase diagram, we combined runs at all temperatures. Uncertainties were estimated by using different combinations of runs. Near the critical point the two peaks overlap significantly, which makes direct determination of the coexisting densities difficult. Compared with the calculations of Brovchenko *et al.*,[44] our phase diagram encompasses the density range corresponding to the three liquid-liquid transitions reported by these authors for the truncated ST2 model, as well as both of the liquid-liquid transitions for ST2 water with reaction field treatment of long-range electrostatic interactions reported therein. In both cases, our low-density branch has approximately the same density as the corresponding branch of their lowest-density transition, whereas our high-density branch has approximately the same density as the corresponding branch of their highest-density transition. In short, we did not see multiple liquid-liquid transitions in the density range $0.9\ \text{g/cm}^3 \leq \rho \leq 1.2\ \text{g/cm}^3$.

The internal energy of each phase at coexistence is shown in Fig. 5. Within the temperature range studied, the internal energy of the high-density phase is approximately 2.5 kJ/mol higher than that of the low-density phase, which corresponds approximately to 1/10 of a hydrogen bond. This is a small energy difference, especially when considered in relation to the appreciable structural differences between water's high-density and low-density amorphous phases.[65]

By further investigating the histograms with the density range extended to 1.30 g/cm$^3$, we found no sign of additional phase transitions. Figure 6 shows the $\mu^*$ versus $\langle\rho\rangle$ isotherms at different temperatures across the entire density range studied, $0.90 \leq \rho \leq 1.3$ g/cm$^3$. The isotherms display strong curvature changes as a result of the liquid-liquid critical point. The abruptness of the density change becomes more pronounced as the temperature decreases. It can be seen that even at a temperature about 7 K higher than the

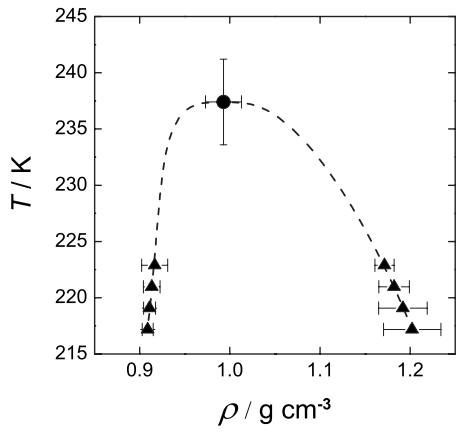


FIG. 4. Liquid-liquid coexistence in ST2 water. The circle denotes the critical point, and triangles show phase coexistence, determined by histogram-reweighting. Error bars were determined by doubling the standard deviation over independent combinations of runs. The dashed line is a guide to the eye obtained by fitting the data to scaling relations near the critical point.

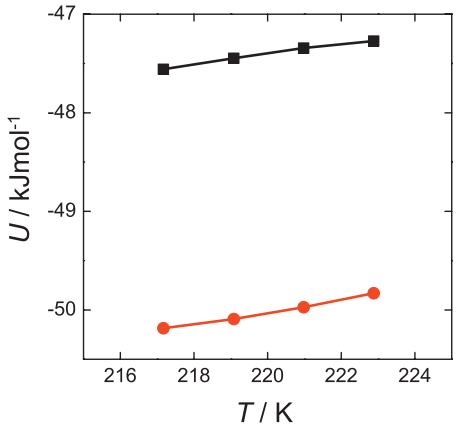


FIG. 5. Configurational energy $U$ of each phase at coexistence. Squares: high-density liquid; circles: low-density liquid. Lines are drawn through points for visual clarity.

critical point ($T$=244.2 K), a curvature change still persists. The two subcritical isotherms ($T$=230 K, 217.2 K) show an abrupt density change due to the first-order phase transition, as well as the rounding characteristic of phase transitions in finite systems. At $T$=217.2 K, the chemical potential changes smoothly as a function of the density within the density range 1.22 g/cm$^3$ $\leq \rho \leq$ 1.3 g/cm$^3$, in a manner that is inconsistent with the existence of an additional phase transition. In this region, the corresponding histogram exhibits only one sharp peak, and this peak gradually shifts to higher density as the chemical potential increases (Fig. 7). This finding further excludes the possibility that additional phase transitions may occur in the density range 1.2 g/cm$^3$ $\leq \rho \leq$ 1.3 g/cm$^3$. Our results suggest that this additional liquid-liquid critical point either does not exist for the ST2 model with Ewald sum treatment of long-range Coulombic interactions, or is located at considerably lower temperatures.

## IV. CONCLUSIONS

In this work we have used histogram-reweighting grand-canonical Monte Carlo simulations of the ST2 model of water[40] with Ewald sum treatment of long-range Coulombic interactions, to study low-temperature first-order phase transitions between metastable liquid phases. The calculations were motivated by reports in the literature of multiple liquid-liquid transitions in the ST2 model.[43,44]

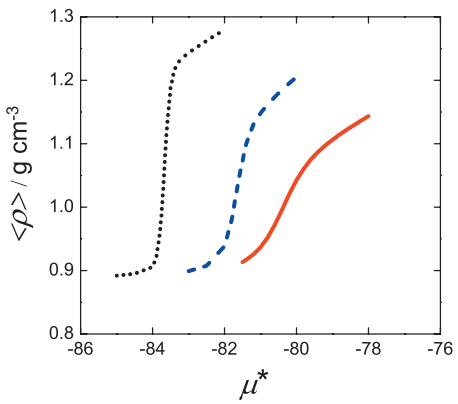


FIG. 6. Isotherms of average density, $\langle\rho\rangle$, versus chemical potential, $\mu^*$. Red solid line: 244.2 K; blue dashed line: 230.0 K; black dotted line: 217.2 K.

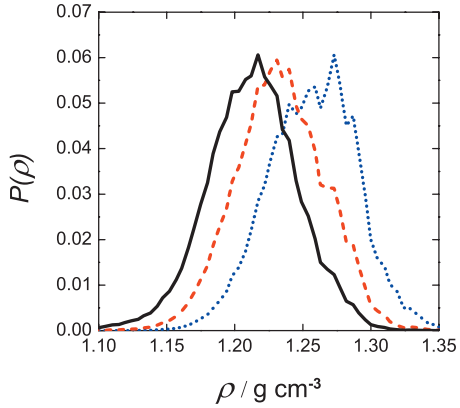


FIG. 7. Density histograms for ST2 water at $T$=217.2 K. Black solid line: $\mu^*$=−83.5; red dashed line: $\mu^*$=−83.0; blue dotted line: $\mu^*$=−82.5.

We have located the liquid-liquid critical point of this model with considerably greater precision than had hitherto been possible. We find reasonable agreement with the calculations of Poole *et al.*,[37] but a considerably lower critical temperature (237 ± 4 K) than the one reported by Brovchenko *et al.*, both for ST2 with simple truncation of electrostatic interactions (~290 K > $T_c$ > 275 K),[43] and for ST2 with reaction field treatment of long-range electrostatic interactions (≳260 K) (Ref. 44) (see Table I).

We also investigated the model's low-temperature, high-density behavior and found no evidence of additional liquid-liquid phase transitions for $T$>217 K. This discrepancy with the results of Brovchenko *et al.*, according to whom there are three liquid-liquid transitions in ST2 water with simple truncation of electrostatic interactions,[43] and two in ST2 with reaction field treatment of long-range Coulombic forces,[44] raises interesting questions that deserve further investigation. In particular, it is important to understand whether these differences are caused by the treatment of electrostatic interactions, the suppression of fluctuations in restricted ensemble calculations,[51] or both. In the former case, this would point to a major sensitivity of low-temperature phase equilibrium calculations to the treatment of long-range electrostatics, the origin and extent of which is not well understood at present. In the second scenario, the discrepancies would constitute clear evidence of the errors incurred in phase equilibrium calculations by suppressing fluctuations in order to constrain a system to remain homogeneous across the coexistence region.

Our results add to the growing number of experiments,[15–22] simulations,[14,34–39,61] and calculations[66–68] that provide evidence of liquid-liquid immiscibility in pure substances. Whether this phenomenon actually occurs in supercooled water is a question, the unambiguous answer to which remains a major challenge in condensed matter physics.

## ACKNOWLEDGMENTS

PGD gratefully acknowledges the support of the National Science Foundation (Collaborative Research in Chem-

istry Grant No. CHE 0404699). Additional support was provided by the Princeton Center for Complex Materials (PCCM), a National Science Foundation funded Materials Research Science and Engineering Center, Award No. DMR-0819860.

[1] F. Franks, *Water: A Matrix for Life*, 2nd ed. (Royal Society of Chemistry, Cambridge, 2000).
[2] P. G. Debenedetti, J. Phys.: Condens. Matter **15**, R1669 (2003).
[3] C. Lobban, J. L. Finney, and W. F. Kuhs, Nature (London) **391**, 268 (1998).
[4] V. F. Petrenko and R. W. Whitworth, *Physics of Ice* (Oxford University Press, Oxford, 1999).
[5] P. H. Poole, F. Sciortino, U. Essmann, and H. E. Stanley, Nature (London) **360**, 324 (1992).
[6] O. Mishima, L. D. Calvert, and E. Whalley, Nature (London) **314**, 76 (1985).
[7] O. Mishima, J. Chem. Phys. **100**, 5910 (1994).
[8] R. J. Speedy, J. Phys. Chem. **86**, 982 (1982).
[9] S. Sastry, P. G. Debenedetti, F. Sciortino, and H. E. Stanley, Phys. Rev. E **53**, 6144 (1996).
[10] P. F. McMillan, M. Wilson, M. C. Wilding, D. Daisenberger, M. Mezouar, and G. N. Greaves, J. Phys.: Condens. Matter **19**, 415101 (2007).
[11] P. H. Poole, T. Grande, C. A. Angell, and P. F. McMillan, Science **275**, 322 (1997).
[12] J. L. Yarger and G. H. Wolf, Science **306**, 820 (2004).
[13] P. F. McMillan, J. Mater. Chem. **14**, 1506 (2004).
[14] S. Sastry and C. A. Angell, Nature Mater. **2**, 739 (2003).
[15] P. F. McMillan, M. Wilson, D. Daisenberger, and D. Machon, Nature Mater. **4**, 680 (2005).
[16] M. Durandurdu and D. A. Drabold, Phys. Rev. B **66**, 041201 (2002).
[17] Y. Katayama, Y. Inamura, T. Mizutani, M. Yamakata, W. Utsumi, and O. Shimomura, Science **306**, 848 (2004).
[18] C. Sanloup, E. Gregoryanz, O. Degtyareva, and M. Hanfland, Phys. Rev. Lett. **100**, 075701 (2008).
[19] A. Ha, I. Cohen, X. Zhao, M. Lee, and D. Kivelson, J. Phys. Chem. **100**, 1 (1996).
[20] A. Hédoux, Y. Guinet, and M. Descamps, Phys. Rev. B **58**, 31 (1998).
[21] R. Kurita and H. Tanaka, Science **306**, 845 (2004).
[22] H. Tanaka, R. Kurita, and H. Mataki, Phys. Rev. Lett. **92**, 025701 (2004).
[23] O. Mishima and H. E. Stanley, Nature (London) **392**, 164 (1998).
[24] A. Faraone, L. Liu, C.-Y. Mou, C.-W. Yen, and S.-H. Chen, J. Chem. Phys. **121**, 10843 (2004).
[25] L. Liu, S.-H. Chen, A. Faraone, C.-W. Yen, and C.-Y. Mou, Phys. Rev. Lett. **95**, 117802 (2005).
[26] F. Mallamace, M. Broccio, C. Corsaro, A. Faraone, U. Wanderlingh, L. Liu, C.-Y. Mou, and S.-H. Chen, J. Chem. Phys. **124**, 161102 (2006).
[27] L. Liu, S.-H. Chen, A. Faraone, C.-W. Yen, C.-Y. Mou, A. Kolesnikov, E. Mamontov, and J. Leao, J. Phys.: Condens. Matter **18**, S2261 (2006).
[28] F. Mallamace, M. Broccio, C. Corsaro, A. Faraone, L. Liu, C.-Y. Mou, and H.-S. Chen, J. Phys.: Condens. Matter **18**, S2285 (2006).
[29] F. Mallamace, M. Broccio, C. Corsaro, A. Faraone, D. Majolino, V. Venuti, L. Liu, C.-Y. Mou, and S.-H. Chen, Proc. Natl. Acad. Sci. U.S.A. **104**, 424 (2007).
[30] D. Liu, Y. Zhang, C.-C. Chen, C.-Y. Mou, P. H. Poole, and S.-H. Chen, Proc. Natl. Acad. Sci. U.S.A. **104**, 9570 (2007).
[31] F. Mallamace, C. Branca, M. Broccio, C. Corsaro, C.-Y. Mou, and S.-H. Chen, Proc. Natl. Acad. Sci. U.S.A. **104**, 18387 (2007).
[32] F. Mallamace, C. Corsaro, M. Broccio, C. Branca, N. González-Segredo, J. Spooren, and S.-H. Chen, Proc. Natl. Acad. Sci. U.S.A. **105**, 12725 (2008).
[33] J. Swenson, Phys. Rev. Lett. **97**, 189801 (2006).
[34] S. Harrington, S. Zhang, P. H. Poole, F. Sciortino, and H. E. Stanley, Phys. Rev. Lett. **78**, 2409 (1997).
[35] M. Yamada, H. E. Stanley, and F. Sciortino, Phys. Rev. E **67**, 010202 (2003).
[36] M. Yamada, S. Mossa, H. E. Stanley, and F. Sciortino, Phys. Rev. Lett. **88**, 195701 (2002).
[37] P. H. Poole, I. Saika-Voivod, and F. Sciortino, J. Phys.: Condens. Matter **17**, L431 (2005).
[38] D. Paschek, Phys. Rev. Lett. **94**, 217802 (2005).
[39] P. Jedlovszky and R. Vallauri, J. Chem. Phys. **122**, 081101 (2005).
[40] F. H. Stillinger and A. Rahman, J. Chem. Phys. **60**, 1545 (1974).
[41] S. Harrington, P. H. Poole, F. Sciortino, and H. E. Stanley, J. Chem. Phys. **107**, 7443 (1997).
[42] H. J. C. Berendsen, J. R. Grigera, and T. P. Straatsma, J. Phys. Chem. **91**, 6269 (1987).
[43] I. Brovchenko, A. Geiger, and A. Oleinikova, J. Chem. Phys. **118**, 9473 (2003).
[44] I. Brovchenko, A. Geiger, and A. Oleinikova, J. Chem. Phys. **123**, 044515 (2005).
[45] W. L. Jorgensen, J. Chandrasekhar, J. D. Madura, R. W. Impey, and M. L. Klein, J. Chem. Phys. **79**, 926 (1983).
[46] M. W. Mahoney and W. L. Jorgensen, J. Chem. Phys. **112**, 8910 (2000).
[47] I. G. Tironi, R. Sperb, P. E. Smith, and W. F. van Gunsteren, J. Chem. Phys. **102**, 5451 (1995).
[48] C. L. Brooks III, B. M. Pettitt, and M. Karplus, J. Chem. Phys. **83**, 5897 (1985).
[49] P. E. Smith and B. Montgomery Pettitt, J. Chem. Phys. **95**, 8430 (1991).
[50] P. Ewald, Ann. Phys. **369**, 253 (1921).
[51] D. S. Corti and P. G. Debenedetti, Chem. Eng. Sci. **49**, 2717 (1994).
[52] A. M. Ferrenberg and R. H. Swendsen, Phys. Rev. Lett. **63**, 1195 (1989).
[53] D. Frenkel and B. Smit, *Understanding Molecular Simulation: From Algorithms to Applications*, 2nd ed. (Academic, New York, 2002).
[54] A. Z. Panagiotopoulos, J. Phys.: Condens. Matter **12**, R25 (2000).
[55] N. B. Wilding and A. D. Bruce, J. Phys.: Condens. Matter **4**, 3087 (1992).
[56] N. B. Wilding, Phys. Rev. E **52**, 602 (1995).
[57] J. J. Potoff and A. Z. Panagiotopoulos, J. Chem. Phys. **109**, 10914 (1998).
[58] A. Z. Panagiotopoulos, V. Wong, and M. A. Floriano, Macromolecules **31**, 912 (1998).
[59] P. J. Lenart and A. Z. Panagiotopoulos, J. Phys. Chem. B **110**, 17200 (2006).
[60] G. Orkoulas and A. Z. Panagiotopoulos, J. Chem. Phys. **110**, 1581 (1999).
[61] C. W. Hsu, J. Largo, F. Sciortino, and F. W. Starr, Proc. Natl. Acad. Sci. U.S.A. **105**, 13711 (2008).
[62] M. M. Tsypin and H. W. J. Blote, Phys. Rev. E **62**, 73 (2000).
[63] V. I. Harismiadis, J. Vorholz, and A. Z. Panagiotopoulos, J. Chem. Phys. **105**, 8469 (1996).
[64] K. Binder, Eur. Phys. J. B **64**, 307 (2008).
[65] J. L. Finney, A. Hallbrucker, I. Kohl, A. K. Soper, and D. T. Bowron, Phys. Rev. Lett. **88**, 225503 (2002).
[66] P. H. Poole, F. Sciortino, T. Grande, H. E. Stanley, and C. A. Angell, Phys. Rev. Lett. **73**, 1632 (1994).
[67] T. M. Truskett, P. G. Debenedetti, S. Sastry, and S. Torquato, J. Chem. Phys. **111**, 2647 (1999).
[68] G. Franzese, M. I. Marqués, and H. E. Stanley, Phys. Rev. E **67**, 011103 (2003).